*Tetrahedron* Vol 33, pp 711 to 721. Pergamon Press 1977 Printed in Great Britain

# STUDIES ON THE CIRCULAR DICHROISM OF PENAM AND PENAM SULFOXIDES†

F. S. RICHARDSON and C.-Y. YEH
Department of Chemistry, University of Virginia, Charlottesville, VA 22901, U.S.A.

and

T. C. TROXELL and D. B. BOYD*
Lilly Research Laboratories, Eli Lilly and Company, Indianapolis, IN 46206, U.S.A.

(*Received in USA* 17 *August* 1976; *Received in the UK for publication* 20 *October* 1976)

**Abstract**—Optical rotatory properties of models of 6-aminopenicillanic acid (6-APA) as obtained from earlier molecular orbital and rotatory strength calculations are corroborated by new CD data for 6-APA. The new spectra extend down to 180 nm, revealing a positive Cotton effect near 185 nm due to carbonyl $\pi \rightarrow \pi^*$ transitions. The pH sensitivity of the optical activity of the $\beta$-lactam amide $\pi \rightarrow \pi^*$ and the 203-nm $n \rightarrow \pi^*$ transitions is explainable in terms of electrostatic effects and orbital interactions present in $\alpha$-aminoketones and 4-membered rings which tend to flatten out the $NH_2$ group. These same interactions are responsible for the unusually low $pK_a$ of 4.75 for the amino group; (the carboxyl group of 6-APA has a normal $pK_a$ of 2.5). The previous calculational procedures are extended to the sulfoxides of 6-APA, and the predicted CD spectra are compared to new experimental curves and also to available data for penicillin sulfoxides. The MO's associated with the principal bands are illustrated with the aid of electron density maps. The positive Cotton effect observed and calculated near 230 nm is due to two charge transfer transitions within the asymmetric penam nucleus. Similar to the situation with the unoxidized penams, the sulfoxide of 6-APA displays a very low $pK_a$ for the amino group (3.8) and a change toward a less positive CD band at 202 nm upon protonation of this group.

Molecular orbital (MO) calculations on the electronic structure of penicillin sulfoxides have not previously been described in the literature. These compounds are important in the chemistry of $\beta$-lactam antibiotics.[3] Earlier, the electronic structure[4] and chiroptical properties[1] of the bicyclic penicillin nucleus, penam, were investigated calculationally. Quite reasonable agreement between theory and experiment was achieved. Also, something is known about the electronic structure of sulfoxides of simple model compounds.[5,6] It is the purpose of this paper to extend our MO and chiroptical studies to rather complex sulfoxides, namely, the penam sulfoxides.

We will be presenting new experimental UV absorption, CD, and $pK_a$ data for the parent penicillin structure, 6-aminopenicillanic acid (6-APA, **1**). Whereas previous spectra of this compound and other penicillins have been for $\lambda \geq 195$ nm, our results extend the spectra down to 180 nm and allow a previously unobserved band to be detected. One of the $pK_a$'s of 6-APA is rather unusual, although not much note of it seems to have been made in the literature. A very nice explanation for this $pK_a$ and for the pH sensitivity of the spectral properties is afforded by the MO results because both stem from special orbital interactions between the amino group and the $\beta$-lactam CO group.

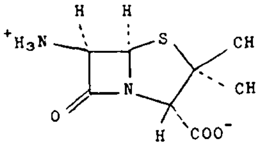

1

The same calculational method which works well in predicting the electronic structure of penams will be applied to the penam sulfoxides. Several conformational and configurational variables will be examined. The calculational results, along with earlier experimental CD data on penicillin sulfoxides, will be compared to UV and CD measurements on an authentic sample of the $\beta$ sulfoxide of 6-APA, 6-APA (S)-sulfoxide (**2**).

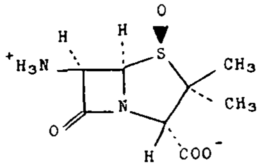

2

Mutual agreement for the characteristic 230-nm CD band is obtained. The orbitals responsible for this and other optically active transitions will be shown with electron density maps. These orbitals can also be expected to play a role in the chemistry of the penicillin sulfoxides.

## EXPERIMENTAL

The MO method employed earlier, that is, the extended Hückel (EH) method,[7,8] is applied to the penam sulfoxides. Orbital and other parameters for this method are identical to those used before.[1,4] The LCAO-MO coefficients for the high-lying filled and low-lying empty MO's are used along with their eigenvalues, $\epsilon$, and the virtual orbital approximation to evaluate the spectral properties. These include the excitation energies in wavelength $\lambda$, the reduced rotatory strengths [R], dipole strengths D, dissymmetry factors g, and oscillator strengths f for each

---

†Paper VI of the series "Electronic Structures of Cephalosporins and Penicillins" (see Ref. 1 for Part V), and paper XIII of the series "Mapping Electron Density in Molecules" (see Ref. 2 for Part XII).

transition. Transition moment integrals are fully evaluated between all the Slater-type orbital basis functions. The rotatory strengths and transition energies can be combined with an assumption of gaussian-shaped bands to compute molar ellipticities. Definitions of these quantities and other details of the procedure for our quantum mechanical computer experiments can be found elsewhere.[1,9] Based on our previous experience, an exponential half-width band parameter $\delta$ of 20 nm works well for penams and will be used here too.

Molecular geometries for the EH calculations on the model penam sulfoxides are based on those previously employed for penam.[1] The only new feature is the addition of oxygen to either the $\alpha$ or $\beta$ face of sulfur to make, respectively, the R(3) or S(4) sulfoxide. The oxygen is positioned[5] with an S–O bond length of 1.47 Å and C–S–O bond angles of 106°. EH calculations were done for both the zwitterionic and unionized (6-NH$_2$, 3-COOH) forms of 3 and 4. However, in the interest of saving computer time, the chiroptical calculations were done on only the zwitterions, since these are more relevant to the physically observed forms. Two envelope-type conformations of the 5-membered ring in penam were considered: one with the 3$\alpha$-COO axial (ax.), and the other with it equatorial (eq.). In light of earlier experience[1] indicating little effect of rotation of the plane of the carboxyl group about the C–COO bond, this structural variable was held fixed (at a crystallographically observed dihedral angle that we have denoted[1] 0°).

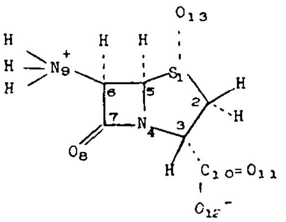

**3**

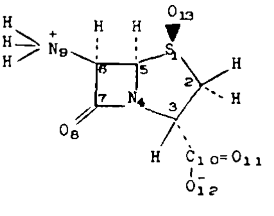

**4**

Electron density maps were computed for the three highest occupied MO's of one of the penam model structures, 6-NH$_2$–3$\alpha$-COOH (0°, ax.)-penam (S)-sulfoxide. The EH LCAO–MO coefficients[†] $C_{pm}$ and Slater-type basis function $\chi_p$ enter in the calculation of density according to $D(\mathbf{r}) = 2\Sigma_{p,q}C_{pm}C_{qm}\chi_p(\mathbf{r})\chi_q(\mathbf{r})$ for density at points **r** in selected planes through the molecule.[11] We will be plotting density of the MO's, rather than the MO's themselves, so that the phase[12] of each region of the MO will not be shown in the figures. The phase of the various lobes separated by nodal surfaces may, however, be deduced from the $C_{pm}$ which we will be tabulating.

Additional computer experiments using the new MINDO/3 MO method[13] were carried out to determine the optimized geometries and conformational energies for the three H$_2$N–C rotamers of a simplified $\beta$-lactam model, 1-CH$_3$-3-NH$_2$-azetidin-2-one, **5**. The geometrical parameters (bond lengths, bond angles and dihedral angles) were taken from the standardized $\beta$-lactam values.[14] Hydrogens were added with standard bond lengths and angles,[15] and the N-methyl group was positioned with N$_1$–CH$_3$ 1.43 Å, C$_2$–N$_1$–C 137°, and O=C$_2$–N$_1$–C dihedral angle 0° (cis). The amino hydrogen positions were optimized for the three rotamers. Standard MINDO/3 procedure[‡] and parameters[13] were employed.

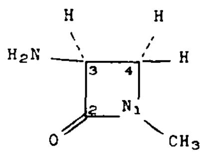

**5**

The compounds 6-APA and 6-APA $\beta$-sulfoxide were obtained within Lilly Research Laboratories. The absolute configuration of the sulfoxide, i.e. S rather than R, was certain, owing to the synthetic route of oxidation.[§] Subsequent reactions using the sulfoxide also proceeded as expected for the $\beta$ rather than the $\alpha$ sulfoxide. Purity of the samples was very high (~99%) as determined by 100 MHz NMR and potentiometric titration.

The p$K_a$'s and pH's of the compounds in aqueous solution were determined with a Lilly-built automatic titrator, which utilizes a Corning Model 12 research pH meter. UV absorption measurements were run on a thoroughly N$_2$ purged Cary 118CX using an $\epsilon$ data display mode. The reference cell and baseline runs were made with aqueous solvent of exactly the same composition and pH as used in the penam solutions. The CD spectra were run on a modified JASCO J-40AS circular dichrometer with data displayed in the $\Delta\epsilon$ mode. Dried d-10-camphor-sulfonic acid (Eastman Organic Chemicals), for which $\Delta\epsilon_{290} = 2.357$, was used for calibration.[16] Spectral measurements were made at ambient temperature on 0.34–0.45 mg/ml aqueous solutions in 0.05 and 1 cm cells. The pH's were either buffered (e.g. $10^{-3}$ M phosphate) or were sufficiently stable within the pH region of interest so as to define the ionization state. The experiments were designed to avoid serious decomposition problems. Checks on the samples indicated that this was mostly successful with the most serious problem occurring in the 0.1 M HClO$_4$ 6-APA $\beta$ sulfoxide solution, where decomposition may have lowered the CD peaks by only 2–3%.

## RESULTS AND DISCUSSION

Let us begin by examining the p$K_a$, UV absorption, and CD data which we have obtained for 6-APA. The results confirm and extend what was previously known about this compound and also corroborate our previous predictions[1] about the penam chromophore.

Titration of 6-APA reveals a fairly normal p$K_a$ of 2.5 for the carboxyl group, but a curiously low p$K_a$ of 4.75 for the amino group. The p$K_a$'s of the $\alpha$-carboxyl group of divalent peptides are ordinarily observed in the range 2.8–3.5, whereas $\alpha$-amino group p$K_a$'s of these compounds are usually in the range 7.2–9.1.[17] (Later in this section we will present an explanation for the low basicity of the amino group of 6-APA.) The p$K_a$'s suggest that appropriate pH's for observing the high pH (6-NH$_2$, 3-COO$^-$), zwitterionic (6-NH$_3^+$, 3-COO$^-$), and low pH (6-NH$_3^+$, 3-COOH) forms of 6-APA are 7.35, 3.9 and 1.1, respectively. The absorption and CD spectral data at these pH's are given in Fig. 1.

The absorption spectra of 6-APA at pH's 3.9 and 7.35 are not too revealing, but they do show a slight shoulder near 205 nm, which is very close to the 200-nm $\lambda_{max}$ predicted[1] for the $\beta$-lactam amide n→$\pi^*$ transition. A relatively high oscillator strength for this transition was calculated,[1] which is consistent with the strong absorption observed in this region (Fig. 1). At pH 1.1 where the carboxyl group is almost fully protonated, the absorption

---

[†] It is of interest to note that no deorthogonalization step is necessary, of course, when one is working with EH MO's because the nonorthogonality of the basis functions is accounted for in the normalization of the wavefunctions. However, when working with neglect-of-differential-overlap wavefunctions this step is essential for obtaining valid density maps (Ref. 10) and is part of the computational procedure employed in our programs (Refs. 2 and 11).

[‡] The computer program for the MINDO/3 calculations is one adapted by D. B. Boyd to incorporate additional new input/output options and to be more efficient. It is based on the IBM double precision FORTRAN version by M. L. Olson, which, in turn, is based on QCPE 279 by M. J. S. Dewar, H. Metiu, P. J. Student, A. Brown, R. C. Bingham, D. H. Lo, C. A. Ramsden, H. Kollmar, P. Weiner and P. K. Bischof. QCPE 279 and 309 are available from the Quantum Chemistry Program Exchange, Indiana University, Bloomington, IN 47401, U.S.A.

[§] T.-S. Chou, unpublished work.

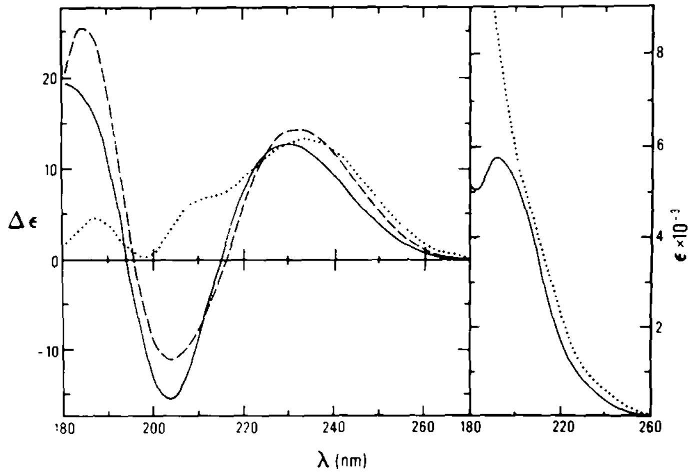

Fig. 1. CD and UV absorption spectra of 6-APA in its three ionization states. The solid curves correspond to the cation in 0.1 M $HClO_4$ (pH = 1.1); the dashed curve to the zwitterion (pH 3.9); and the dotted curves to the anion in $10^{-3}$ M phosphate buffer (pH 7.35). The UV absorption curve of the pH = 3.90 state is not shown because it is very similar to the pH = 7.35 curve, except for a slower increase in the end absorption below 200 nm. Raising the pH above 7.35 does not alter the pH = 7.35 curve.

spectrum changes considerably, so that a broad band at 193 nm emerges which is capable of containing both carboxyl and β-lactam amide $n \rightarrow \pi^*$ transitions. Protonation of the carboxyl group thus diminishes the intensity in the far UV region where carboxyl $\pi \rightarrow \pi^*$ transitions usually occur. This effect has been previously observed, for example, in acetic acid.[18]

The CD curves in Fig. 1 reveal that at low pH's, 6-APA displays a positive Cotton effect near 230 nm and a negative Cotton effect at about 203 nm. These extrema have been reported before.[19,20] Our previous calculations[1] yielded for penam models not only $\lambda_{max}$ and signs of the Cotton effects in good agreement with the observed bands, but even the amplitudes were quite reasonably predicted ($\Delta\epsilon \approx +12.7$ near 236 nm, and $\Delta\epsilon \approx -12.1$ near 199 nm). The calculations could thus be used to confidently assign, in agreement with certain experimental deductions, that the first (230 nm) CD band arises from charge transfer transitions between two occupied MO's localized in the 5-membered ring on S and N (called S n and S-N$\pi$) and the empty, β-lactam amide $\pi^*$ orbital. The second band (203 nm) is associated with the β-lactam amide $n \rightarrow \pi^*$ transition. The CD spectra in Fig. 1 also reveal a third peak which has not been previously reported. This positive band near 185 nm almost certainly arises from the CO $\pi \rightarrow \pi^*$ transitions. MO calculations[1] were not applied to such short wavelengths because the virtual orbital approximation becomes less valid for the higher energy transitions and because the lower energy, occupied MO's are delocalized over many atoms and are not clearly identifiable as part of a specific functionality.

The CD spectrum for the high pH form of 6-APA (Fig. 1) differs in the nature of the second and third Cotton effects from those for the other two ionic forms. Whereas the second Cotton effects in the latter are strong and negative, the high pH form, which has an unprotonated amino group, shows a positive shoulder at about 210 nm. The third Cotton effect (the one due to the $\pi \rightarrow \pi^*$ transitions presumably) is strongly positive for the $NH_3^+$ forms of 6-APA, but is only weakly positive for the $NH_2$ form. We can ask the question why does protonation of the amino group affect so greatly the bands arising from the β-lactam carbonyl group. We can answer this question and the question about the low $pK_a$ of the amino group at the same time.

The amino group and CO group of the β-lactam ring of 6-APA are suitably situated spatially for orbital interaction effects reminiscent of those that have been noted in simpler model structures. In particular, we are interested in interactions of the lone-pair orbital on the amino nitrogen and the orbitals of the 4-membered ring and the CO group. For instance, the lowest empty orbitals of cyclobutane,[21] which are the ones appropriate for interaction with a $\pi$ electron-donating substituent like $NH_2$, can overlap better in a symmetry-allowed way with the $NH_2$ n orbital when the $NH_2$ is oriented in what has been called[21] the bisected conformation **6**, rather than the twisted conformation **7**. In addition to this interaction and probably considerably more important, is the interaction between the CO$\pi^*$ orbital and the amino lone-pair orbital. This type of interaction has been studied in the α-substituted ketones[22] and is known to affect the electronic spectra of α-halo ketones.[23] The origin of this effect can be understood in terms of various concepts, including hyperconjugation (**8**) and orbital overlap and symmetry arguments.[22,23] These latter show that the $NH_2$ n orbital prefers to point away from the carbonyl oxygen, but be coplanar with it. For instance, *ab initio* STO-3G calculations[22] establish that the preferred conformation of α-aminoacetaldehyde is **9**.

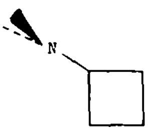

**6**

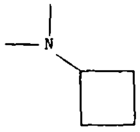

**7**

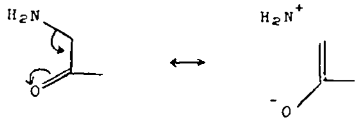

**8**

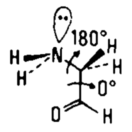

**9**

We can demonstrate that similar, but slightly different, orbital effects are operative in the penam system. MINDO/3 MO calculations were done on the three rotational isomers of **5**. These are shown in **10**, **11** and **12**, which are Newman projections looking down the N–$C_3$ bond of **5**. The energies obtained by optimizing the amino hydrogen positions for these rotamers show that **11** is most stable, **12** is less stable by 0.6 kcal/mole, and **10** is least stable (2.1 kcal/mole less stable than **11**). Thus, the rotamer with the axis of the amino lone-pair orbital roughly parallel to the C=O bond is most stable, and the rotamer with the axis antiparallel to this bond (so that the orbital lobe on the backside of the lone-pair is directed toward the C=O) is second most stable. The reason we believe that **11** and **12** are most stable is that these allow the strongest interactions between the lobes of the $NH_2$ n orbital and the carbonyl $\pi^*$ orbital. Note also that **11** and **12** are well suited for interaction of the $NH_2$ n orbital with the low-lying empty cyclobutane-type orbitals because the $NH_2$ group is approximately in the bisected arrangement.

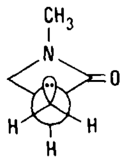

**10**

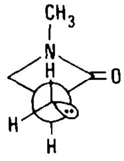

**11**

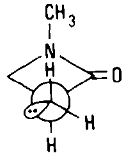

**12**

Pertinent to understanding the CD and p$K_a$ data of 6-APA, the MINDO/3 wavefunctions of **5** show that the amino N 2p atomic orbital (AO) character in the empty amide $\pi^*$ MO is smallest for **10**, increases in **11**, and is biggest in **12**. This orbital mixing has the effect of delocalizing to a small extent the amino lone-pair electrons, so that electron density is drained away from the amino group into the C=O region. The spatial arrangement for the $NH_2$ n···amide $\pi^*$ interaction is depicted in **13** for **11** and **12**. Note that this spatial arrangement differs from that in acyclic $\alpha$-aminoketones, such as $\alpha$-aminoacetaldehyde or glycine, because the $NH_2$ group is situated out of the plane of the CO group. The MINDO/3 MO's also show considerable amino nitrogen AO character in the top three filled orbitals (which include the amide n and $\pi$ orbitals).

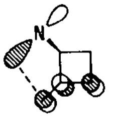

**13**

Reduced electron density on the amino nitrogen, which can be associated with its basicity, is seen in the MINDO/3 net atomic charges: −0.1716 in **10**, −0.1507 in **11** and −0.1656 in **12**. Reduced negative charge in the more stable rotamers can be rationalized in terms of the orbital interactions, as well as in terms of hyperconjugation **8**. Still another qualitative explanation can be cast in terms of Bent's orbital hybridization arguments.[24] The electrons in the $NH_2$ n orbital will prefer to be as close as possible to the positively charged CO carbon because of electrostatic attraction. The negative charge can get closer if the lone-pair hybrid has more N2p AO character. This leaves the N–R bonds with more N2s character, so that the nitrogen will be less pyramidal.

Whatever the rationale, the amino group of 6-APA is expected to have reduced electron density which should show up as a flattening of the amino group in the more abundant rotational isomers. Indeed, in the model structure **5**, the MINDO/3 optimized $NH_2$ geometries have the two C–N–H bond angles at 111° and 115° in **11** and **12**, whereas they are both 111° in **10** and only 104° in $NH_3$. In terms of the dihedral angle necessary to twist one H of the $H_2N$–R group into the other's position, the values are 120° in **12** and 118° in **11** *versus* 116° in **10** and 109° in $NH_3$. Thus, the $NH_2$ group of 6-APA will definitely be slightly less pyramidal in its more stable rotamers than ordinary amino groups.

As we have stated, the same orbital effects which result in the intriguing p$K_a$ and geometrical features of 6-APA also contribute to the properties of the CD bands for the $\beta$-lactam amide $n \rightarrow \pi^*$ and $\pi \rightarrow \pi^*$ transitions. One *other* factor which should not be overlooked in interpreting the CD spectra is the redistribution of the static charge around the amide group upon protonation of the proximal 6-amino group of 6-APA. An asymmetric static charge distribution results in rotatory strength by the one-electron (Condon, Altar and Eyring) mechanism.[25] By this mechanism the $n \rightarrow \pi^*$ and $\pi \rightarrow \pi^*$ $\beta$-lactam amide transitions develop into equal, but oppositely signed, rotatory strengths. Because such a couplet is apparent in the low pH curves of Fig. 1, the one-electron mechanism does seem to be important. Moreover, this interpretation lends further support to the assignments of these two bands that we have given above.

Having now compared the experimental and theoretical electronic spectra of 6-APA and shown them to be harmonious, let us next consider the penam sulfoxides. Experimental UV and CD data on the sulfoxides of 6-APA have not been available previously. Our spectra for **2** are presented in Fig. 2. They have been collected at pH's 1.1, 3.23 and 6.1 because titration reveals that the p$K_a$ of the carboxyl group is below 2.5 (probably 1.8–2.0) and the p$K_a$ of the amino group is 3.8. Thus, the p$K_a$'s for these groups are even lower in **2** than in **1**. The low p$K_a$ of the amino group in **2** is most likely due to an enhancement of the orbital interactions we have already discussed for 6-APA. The low p$K_a$ of the carboxyl group presumably stems from the electrostatic field effects[26] of the $S^+$–$O^-$ dipole.†

In Fig. 2, one observes that the UV curves for the various ionic states of 6-APA (S)-sulfoxide **2** are quite similar to those for the unoxidized penam (Fig. 1). The dependence of the absorption on pH is also similar. The UV in Fig. 2 does show a slightly more pronounced

---

†Mulliken net atomic charges computed from the EH wavefunctions are −0.99 to −1.00 on the sulfoxide oxygen and +0.94 to +0.96 on sulfur, depending on the conformer.

shoulder near 225 nm. The CD curves of the penam sulfoxide in Fig. 2 show the characteristic 230-nm, positive ($\Delta\epsilon = +12.6$ to $+13.8$, depending on pH) Cotton effect to be very similar to that seen in Fig. 1. Whereas the second CD band near 200 nm is a trough in the low pH forms and a positive shoulder in the high pH form of 6-APA, the second Cotton effect of the $\beta$ sulfoxide is positive, in fact, very positive at all pH's. One consistency, however, between the spectra of the unoxidized and oxidized 6-APA's is that in both cases the second Cotton effect becomes *more* positive (*less* negative) in going from the low to the high pH forms. One final comment about Fig. 2 is that, as noted in its caption, there may be an extremely weak and poorly defined, positive CD band in the 275–305 nm region. Whether this is a real transition of **2**, such as a transition of the sulfoxide chromophore (see below), or is simply due to a trace of impurity (the sample of **2** was slightly yellow) cannot be established at present.

Our experimental CD data on the penam sulfoxide can be compared to data available on the sulfoxides of penicillins. It has been previously pointed out that acylation of the amino group does not seem to drastically affect the characteristic 230-nm penam transition.[1,19,20] Published CD spectra of phenoxymethyl penicillin sulfoxide have only covered the region 210–260.[27] In this region there appears the strong, positive Cotton effect at 227–228 nm ($\Delta\epsilon = +7.1$ to $+10.3$, depending on solvent). Note that this band is very similar in wavelength and intensity to the first Cotton effect of the corresponding penicillin ($\lambda_{max} = 233$–$237$, $\Delta\epsilon = +7.3$ to $+10.9$),[27] and it is also quite similar to what we obtain for the $\beta$ sulfoxide of 6-APA (Fig. 2). There is also a good deal of preliminary UV and CD data on penicillin sulfoxides (both (R) and (S)) which extend to other wavelengths.† These data may be roughly summarized as follows. The $\alpha$-face (R)-sulfoxides give absorption spectra with a broad, low intensity band at about 283 nm, a shoulder in the 230 nm region, and a strong peak near 200 nm. The CD spectra of the (R)-sulfoxides are dominated by a very strong, positive Cotton effect near 200 nm and a less, but still strong peak near 230 nm; there are also a weak trough in the 255–265 nm region and a still weaker negative Cotton effect near 285 nm. The $\beta$-face (S)-sulfoxides of penicillin absorb weakly near 272 nm and strongly near 207 nm with a slight shoulder in the vicinity of 230 nm. The CD spectra of the (S)-sulfoxides, as with the (R)-sulfoxides, are characterized by a very strong, positive Cotton effect near 202 nm and a secondary strong peak near 230; other extrema are a trough in the 255–265 nm region and a peak near 285 nm, both of which are relatively very weak. Thus, one qualitative difference between the (R)- and (S)-sulfoxides seems to be that the rotatory strength is negative in the 280–290 nm region in the former, but is positive in the latter. Except for the long wavelength 275–305 nm region, where our 6-APA (S)-sulfoxide spectra are inconclusive, the CD curves for the penicillin sulfoxides resemble quite closely the curves in Fig. 2.

The theoretically calculated CD spectra of the penam sulfoxide models **3** and **4** are shown in Figs. 3 and 4. The (R)-sulfoxides (Fig. 3) give a weak, negative Cotton effect at 266–268 nm, a strong, positive extremum at 230–235 nm, and a negative band slightly below 200 nm. Flipping the penam model **3** between carboxyl-axial and equatorial conformers does not greatly alter the spectrum, although the first and third bands are slightly weakened at the expense of the second in the equatorial form. The (S)-sulfoxides (Fig. 4) do not show a negative extremum at long wavelengths, but the positive Cotton effect near 235 nm and the negative Cotton effect at about 200 nm are similar to those for the (R)-sulfoxides. In the (S)-sulfoxides, the 230-nm band is predicted to become

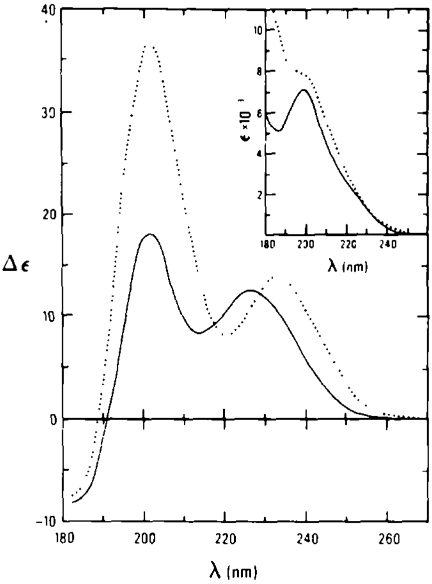

Fig. 2. CD and UV absorption spectra of 6-APA (S)-sulfoxide. The solid curves correspond to the 0.1 M $HClO_4$ (pH = 1.1) aqueous solution, where 80–90% of the compound is in the cationic form; and the dotted curves to the unbuffered solution (pH 6.1–6.6), where more than 99% of the compound is in the anionic form. Not shown are the curves for the unbuffered pH = 3.23 solution, where the composition is roughly 80% zwitterion and 20% anion; the CD curve at pH = 3.23 is very similar to that of the cation, except for a positive minimum at 187 nm instead of the cation's negative band; the UV absorption curve at pH 3.23 is similar to that of the anion. In all three pH's where the spectra were measured, there is also very weak, positive amplitude ($\Delta\epsilon$ less than $+0.02$) in the region 275–305 nm.

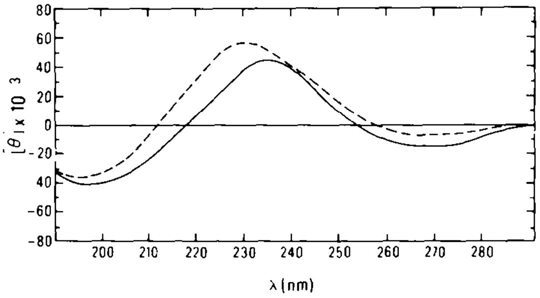

Fig. 3. Predicted CD spectra of $6\text{-}NH_3^+\text{-}3\alpha\text{-}COO^-$-penam (R)-sulfoxides. The solid curve corresponds to the conformer with the carboxyl group axial; the dashed curve to the equatorial conformer. Both curves were computed with a half-bandwidth parameter of 20 nm using the 10 lowest energy transitions. The difference in extinction coefficients for left and right circularly polarized light is related to molar ellipticity by $\Delta\epsilon \approx [\theta]/3298$, where $\Delta\epsilon$ is in $l.\ mole^{-1}\ cm^{-1}$ and $[\theta]$ is expressed in $deg\ cm^2\ dmol^{-1}$.

---

†M. M. Marsh, unpublished work; R. D. Miller, unpublished work.

Table 1. Calculated spectral properties for the ten lowest energy transitions of 6-$NH_3^+$-3-$COO^-$(ax., 0°)-penam (R)-sulfoxide[a]

| Transition | λ | [R] | \|g\| | D | f |
|---|---|---|---|---|---|
| 1 (29-30) | 259.3 | -28.92 | 0.0068 | 1.5692 | 0.0284 |
| 2 (29-31) | 247.7 | -26.66 | 0.0064 | 1.5417 | 0.0293 |
| 3 (28-30) | 244.2 | 28.44 | 0.0121 | 0.8713 | 0.0168 |
| 4 (28-31) | 233.9 | 88.02 | 0.0120 | 2.7238 | 0.0548 |
| 5 (27-30) | 220.5 | -9.70 | 0.0002 | 15.1426 | 0.3229 |
| 6 (27-31) | 212.0 | -12.62 | 0.0028 | 1.6771 | 0.0372 |
| 7 (29-32) | 208.9 | 8.47 | 0.0017 | 1.8849 | 0.0424 |
| 8 (26-30) | 206.4 | 36.33 | 0.0009 | 15.1737 | 0.3457 |
| 9 (28-32) | 199.0 | -123.32 | 0.0198 | 2.3062 | 0.0545 |
| 10 (26-31) | 198.9 | -12.49 | 0.0020 | 2.3265 | 0.0550 |

[a] Units are nm for wavelength λ, 100·Debye·Bohr magnetons/molecule for the reduced rotatory strength [R], $10^{-36}$ esu$^2$·cm$^2$/molecule for dipole strength D, and dimensionless for the dissymmetry factor g and the oscillator strength f.

Table 2. EH eigenvalues and MO's of 6-$NH_3^+$-3-$COO^-$(ax., 0°)-penam (R)-sulfoxide[a]

| MO | ε, eV | Large LCAO-MO Coefficients[b] | Mnemonic |
|---|---|---|---|
| 26 | - 5.65 | $+0.45(S_1 3p_x)-0.42(S_1 3d_{z^2})$<br>$+0.44(S_1 3d_{xz})+0.32(S_1 3d_{x^2-y^2})$ | S3d' |
| 27 | - 6.04 | $+0.34(S_1 3p_z)+0.46(S_1 3p_y)$<br>$+0.32(S_1 3d_{z^2})+0.53(S_1 3d_{x^2-y^2})$<br>$-0.33(S_1 3d_{yz})+0.30(O_{13} 2p_y)$ | S3d |
| 28 (NLEMO) | - 6.58 | $-0.35(N_4 2p_x)+0.82(C_7 2p_x)$<br>$-0.32(C_7 2p_y)-0.46(O_8 2p_x)$ | amide π* |
| 29 (LEMO) | - 6.88 | $-0.38(C_{10} 2p_z)-0.78(C_{10} 2p_x)$<br>$+0.42(O_{11} 2p_x)+0.38(O_{12} 2p_x)$ | carboxyl π* |
| 30 (HOMO) | -11.66 | $+0.44(S_1 3p_z)+0.27(S_1 3p_x)$<br>$-0.41(S_1 3p_y)-0.36(O_{13} 2p_z)$<br>$+0.29(O_{13} 2p_y)$ | S-O n |
| 31 (NHOMO) | -11.89 | $+0.28(C_3 2p_y)-0.46(N_4 2p_y)$<br>$+0.25(C_6 2p_z)-0.26(O_8 2p_x)$<br>$+0.28(O_{11} 2p_y)$ | amide N n |
| 32 (NNHOMO) | -12.82 | $-0.33(N_4 2p_x)+0.37(C_6 2p_z)$<br>$+0.47(O_8 2p_z)-0.34(O_8 2p_y)$<br>$-0.25(O_{12} 2p_y)$ | amide n |

[a] α sulfoxide shown in 3; the right-handed coordinate system has $N_4$ at the origin, $C_5$ on the +z axis, and $C_2$ in the ++ quadrant of the xz plane.

[b] LEMO abbreviates lowest empty MO, HOMO highest occupied MO, N next, and NN next to the next; see Ref. 1 or 4 for notation.

weaker, rather than stronger, when the molecule flips to the carboxyl equatorial conformer.

The prediction of a positive Cotton effect near 230 nm is in excellent agreement with the observed spectral data summarized above. We compute $\Delta\epsilon$ to be + 10.4 to + 18.4 for this band depending on the penam conformation and sulfoxide configuration. Experimentally, it is +7.1 to + 13.8, depending on the compound. One wonders if it is valid to associate the weak, negative band predicted near 270 nm for the (R)-sulfoxide models and the broad, positive tail predicted in this region for the carboxyl-equatorial, (S)-sulfoxide model with the weak, long wavelength (280–290 nm) negative and positive bands, respectively, observed in the penicillin sulfoxides. The calculations appear to be yielding the $\lambda_{max}$ for these transitions slightly blue shifted, but the signs of the bands are at least consistent with experiment. On the other hand, the deep trough ($\Delta\epsilon = -7.6$ to $-12.3$) predicted near

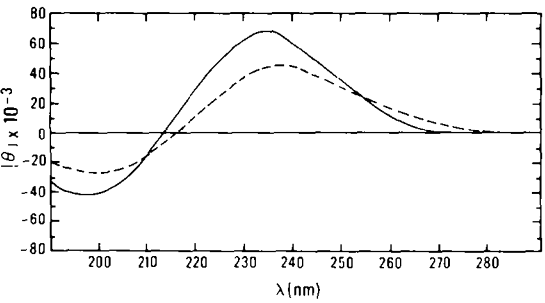

Fig. 4. Predicted CD spectra of 6-$NH_3^+$-3α-$COO^-$-penam (S)-sulfoxides. The solid curve (carboxyl-axial conformer) and dashed curve (carboxyl-equatorial conformer) were computed as in Fig. 3.

200 nm contrasts with the distinctly positive Cotton effect seen experimentally at 203 nm. This discrepancy reflects on the reliability of the approximate nature of our calculations to predict the sign of the β-lactam amide $n \rightarrow \pi^*$ transition satisfactorily. In any case, the prediction of the characteristic 230 nm CD band by our calculations is encouraging, and we will next discuss our calculational results in more detail.

Calculated spectral properties for two of our more stable penam sulfoxide models are presented in Tables 1 and 3, and the corresponding EH MO's are summarized in Tables 2 and 4. It can be seen in the Tables that the main contribution to molar ellipticity in the 270 nm region comes from exciting an electron out of the highest occupied MO into the lowest empty one (based on the

Table 3. Calculated spectral properties for the ten lowest energy transitions of 6-$NH_3^+$-3-COO (eq., 0°)-penam (S)-sulfoxide

| Transition | λ | [R] | \|g\| | D | f |
|---|---|---|---|---|---|
| 1 (29-30) | 254.1 | 19.89 | 0.0050 | 1.4802 | 0.0274 |
| 2 (29-31) | 248.1 | -4.62 | 0.0009 | 1.9406 | 0.0368 |
| 3 (28-30) | 237.5 | 40.68 | 0.0204 | 0.7408 | 0.0147 |
| 4 (28-31) | 232.2 | 51.41 | 0.0083 | 2.2857 | 0.0463 |
| 5 (29-32) | 213.9 | 7.26 | 0.0025 | 1.0868 | 0.0239 |
| 6 (27-30) | 213.0 | -13.52 | 0.0004 | 11.2070 | 0.2474 |
| 7 (27-31) | 208.7 | 48.66 | 0.0035 | 5.1931 | 0.1170 |
| 8 (26-30) | 205.3 | -40.55 | 0.0013 | 11.3189 | 0.2593 |
| 9 (28-32) | 202.0 | -109.42 | 0.0184 | 2.1619 | 0.0503 |
| 10 (26-31) | 201.3 | 38.80 | 0.0039 | 3.7215 | 0.0869 |

Table 4. EH eigenvalues and MO's of 6-$NH_3^+$-3-$COO^-$(eq., 0°)-penam (S)-sulfoxide[a]

| MO | ε, eV | Large LCAO-MO Coefficients | Mnemonic |
|---|---|---|---|
| 26 | - 5.77 | $+0.41(S_1 3p_x)-0.37(S_1 3d_{z2})$<br>$+0.45(S_1 3d_{xz})+0.27(S_1 3d_{x2-y2})$<br>$+0.25(S_1 3d_{yz})$ | S3d' |
| 27 | - 5.98 | $+0.25(S_1 3p_x)-0.52(S_1 3p_y)$<br>$+0.31(S_1 3d_{z2})+0.43(S_1 3d_{x2-y2})$<br>$-0.29(S_1 3d_{yz})+0.40(S_1 3d_{xy})$<br>$-0.25(O_{13} 2p_y)$ | S3d |
| 28 | - 6.59 | $-0.34(N_4 2p_x)+0.82(C_7 2p_x)$<br>$-0.31(C_7 2p_y)-0.46(O_8 2p_x)$ | amide π* |
| 29 (LEMO) | - 6.93 | $+0.31(C_{10} 2p_z)+0.56(C_{10} 2p_x)$<br>$+0.55(C_{10} 2p_y)-0.30(O_{11} 2p_x)$<br>$-0.29(O_{11} 2p_y)-0.27(O_{12} 2p_x)$<br>$-0.27(O_{12} 2p_y)$ | carboxyl π* |
| 30 (HOMO) | -11.81 | $-0.46(S_1 3p_z)+0.31(N_4 2p_y)$<br>$+0.37(O_{13} 2p_z)$ | S-O n |
| 31 | -11.92 | $-0.43(S_1 3p_z)-0.25(C_3 2p_z)$<br>$-0.40(N_4 2p_y)+0.34(O_{13} 2p_z)$ | S-N π |
| 32 | -12.72 | $-0.35(N_4 2p_x)+0.35(C_8 2p_z)$<br>$+0.43(O_8 2p_z)-0.37(O_8 2p_y)$ | amide n |

[a] β-sulfoxide shown in 4; the same coordinate system as described in Table 2 is used.

virtual orbital approximation). The LEMO has carboxyl $\pi^*$ character. The HOMO is seen in Tables 2 and 4 and Fig. 5 to have lone-pair character localized on the S–O moiety. The S–O n MO can be described as the antibonding combination of the free lone-pair lobe on the sulfur and the coplanar, 2p-like lobes on oxygen. This shape is similar to the ones described for simpler sulfoxides.[5,6] We find that the rotatory strength of our longest wavelength transition is negative in the (R)-sulfoxide models and it becomes less negative or positive in the models with the sulfoxide oxygen in the S configuration.

The positive Cotton effect near 230 nm arises mainly from the transitions labeled amide N n→amide $\pi^*$ (Table 2) or S–N $\pi$→amide $\pi^*$ (Table 4). The S–O n→amide $\pi^*$ transition also contributes a significant amount of positive rotatory strength to this characteristic penam band. Rather than being a localized sulfur n→$\sigma^*$ transition,[27] these excitations involve intramolecular charge transfer involving the sulfur *and* amide portions of the molecule. The charge transfer nature of the transitions is similar to that for the S–N $\pi$→amide $\pi^*$ and S n→amide $\pi^*$ transitions in unoxidized penams.[1,28] One difference, however, is that in the sulfoxides, the S–O n MO (Fig. 5) acts as one of the electron donor orbitals. Another difference is that the other donor orbital (the next highest occupied MO) is localized on the $\beta$-lactam N depending on the extent to which other AO's, especially the ones on sulfur, can mix in. In the $\alpha$ sulfoxides, the free lone-pair lobe on sulfur must point "up", so that it cannot mix well with the lone-pair lobes on the $\beta$-lactam N which is directed "down" (see **14**). In fact, the LCAO–MO coefficients of the NHOMO in Table 2 show no significant contribution from the sulfur orbitals. Hence we use the

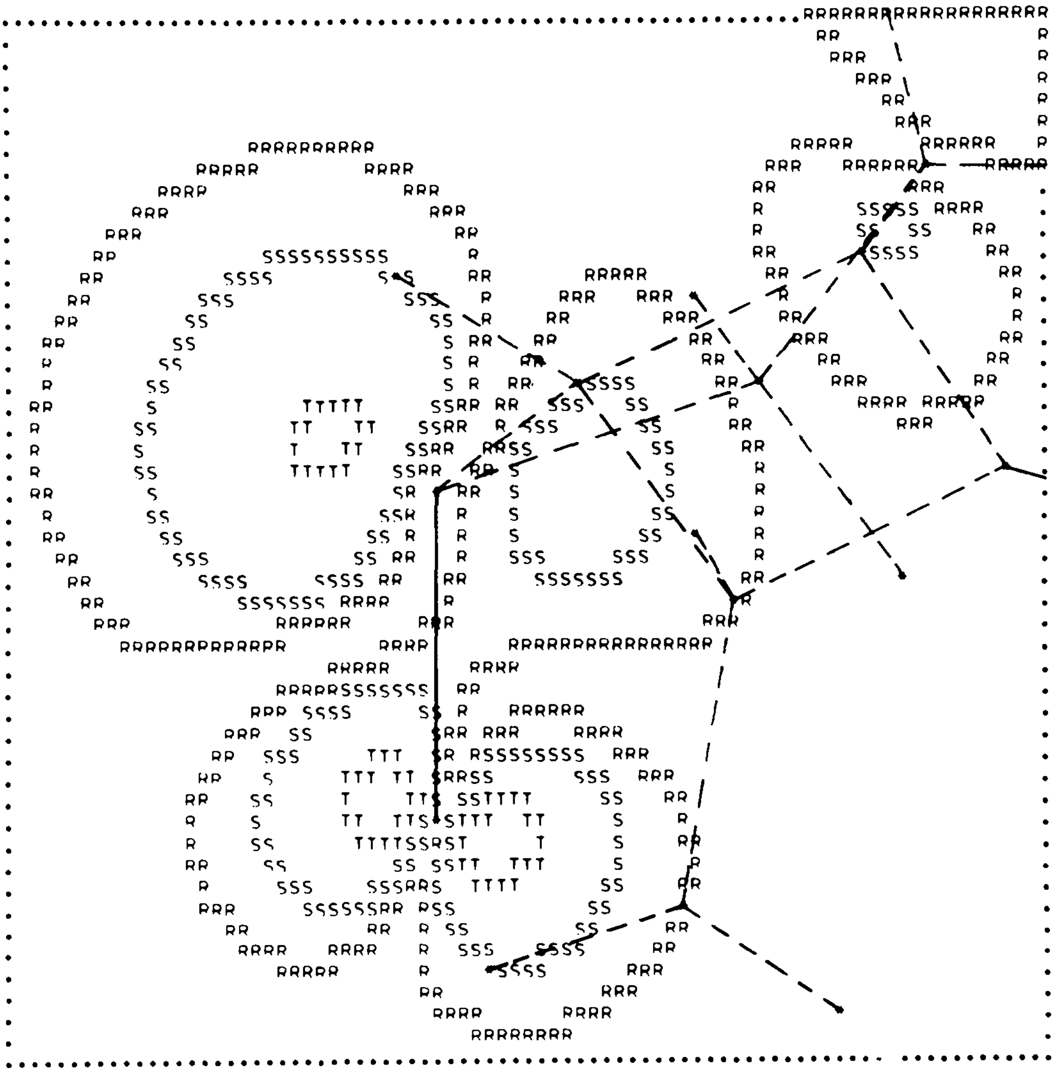

Fig. 5. Electron density map of the HOMO (MO 30) of 7-$NH_2$-3$\alpha$-COOH-penam (S)-sulfoxide from EH calculations. This view shows the density in the plane through $S_1$, $O_{13}$, and $C_3$; $S_1$ lies near the center of the map, $O_{13}$ connected to it by the solid line, and $C_3$ at the upper right. The $\beta$ face of this $\beta$ sulfoxide is toward the bottom of the figure. In this and subsequent maps, positions or projections of positions of nuclei on the plane of the map are denoted by asterisks, and projections of internuclear axes are shown as dashed lines. The maps cover 4.8 × 4.8 Å and have contours labeled T for 0.09, S for 0.009, and R for 0.0009 e/bohr$^3$. Some of the contours appear fused or discontinuous, but this is merely an artifact of the limited resolution of the computer printer. Nodal surfaces between the orbital lobes are not drawn, but they generally intersect the plane of the map between the "R" contours of adjacent lobes. The phase of the MO's generally change sign across these nodes.

label "amide N n" for the NHOMO in the $\alpha$ sulfoxides. On the other hand, in the $\beta$ sulfoxides, the large lobes on sulfur and nitrogen point toward the same side (see **15**) and mix in a bonding fashion. Hence, the label "S–N $\pi$".

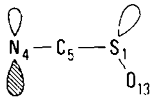

**14**

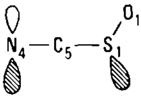

**15**

The electron density map of this MO in Fig. 6 shows that some amide oxygen character also mixes in, but by comparing this electron density map with the one for the amide n MO (in Fig. 7), one notes that the qualitative appearance of the two is different. Thus, our amide N n and amide n MO's should not be confused, and the 230-nm Cotton effect is contributed to by the former, and not the latter. The penam MO shapes are not directly comparable to those for formamide[12] because the latter molecule is unstrained and has a plane of symmetry.

The trough in our calculated CD spectra near 200 nm is seen in the tables to arise from the $\beta$-lactam amide $n \rightarrow \pi^*$ transition. The rotatory strength is very large and negative as calculated for the unoxidized penams.[1] Although apparently wrong for penam sulfoxides, the negative sign of the $n \rightarrow \pi^*$ transition is appropriate for unoxidized penams,[19,20] and has also been used to identify the stereochemistry of substituted monocyclic $\beta$-lactams.[29] In the latter connection, it is worthwhile to remark that the positive sign of both Cotton effects seen in our spectra for the 6-APA $\beta$ sulfoxide (Fig. 2) seems to require a refinement of a proposed[29] lactam rule.

Oscillator strengths of the S–O $n \rightarrow$ empty S3d transitions in Tables 1 and 3 are puzzling because of their large size. Previous calculations[1,4] showed that the localized transitions of unoxidized divalent sulfides give rise to only rather weak absorptions. The large values for the localized sulfoxide transitions are not supported by the UV data in Fig. 2.

We conclude with a few remarks about the conformational energies for the penam sulfoxides that we obtain from the EH MO calculations. There is ample evidence[30] that the penicillin sulfoxides exist preferentially in a conformation with the $3\alpha$ substituent in an

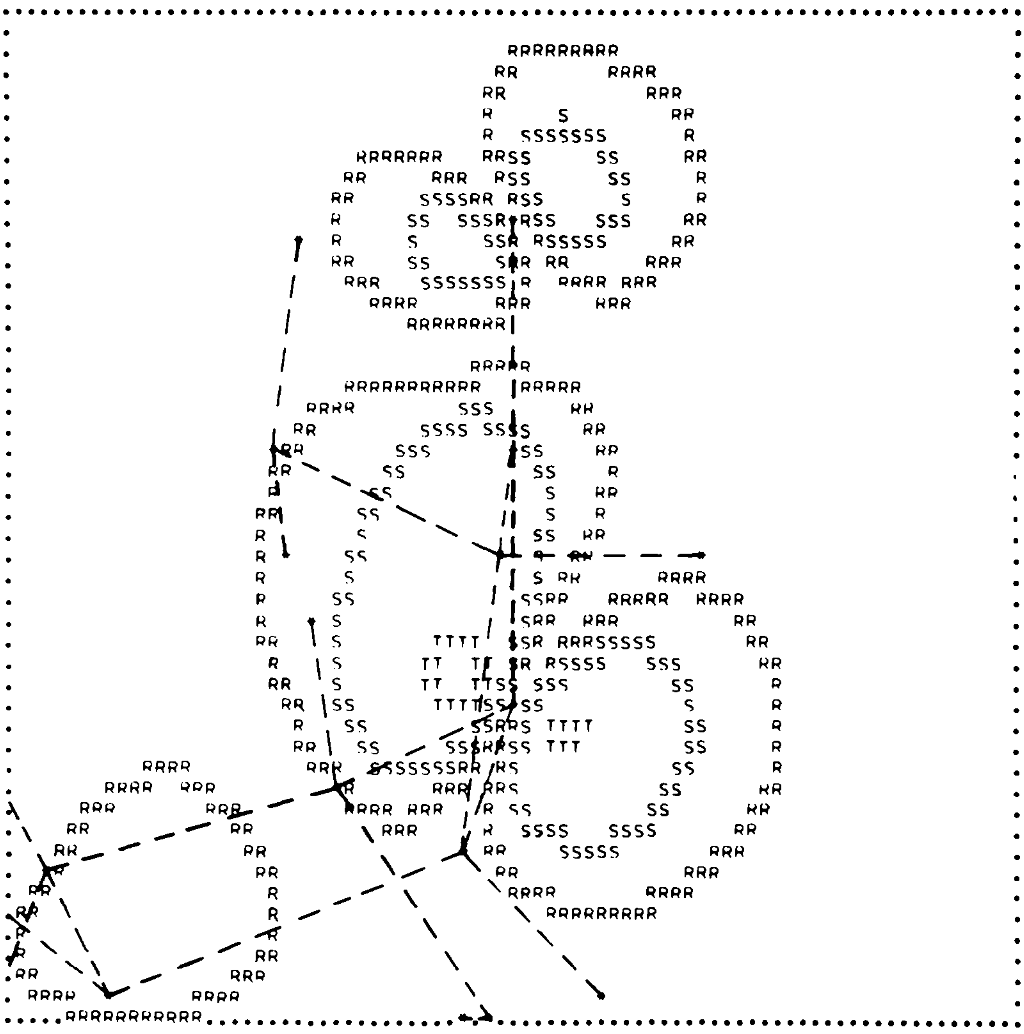

Fig. 6. Electron density map of the NHOMO (MO 31) of 7-$NH_2$-$3\alpha$-COOH-penam (S)-sulfoxide from EH calculations. This view shows the density in the plane through $N_4$ and $O_8$ which is perpendicular to the plane passing through $N_4$, $C_7$, and $O_8$. $N_4$ is in the lower center (between the "T" contours), $C_7$ is near the center, and $O_8$ is at the upper center of the map. The $\beta$ face of the molecule is toward the left.

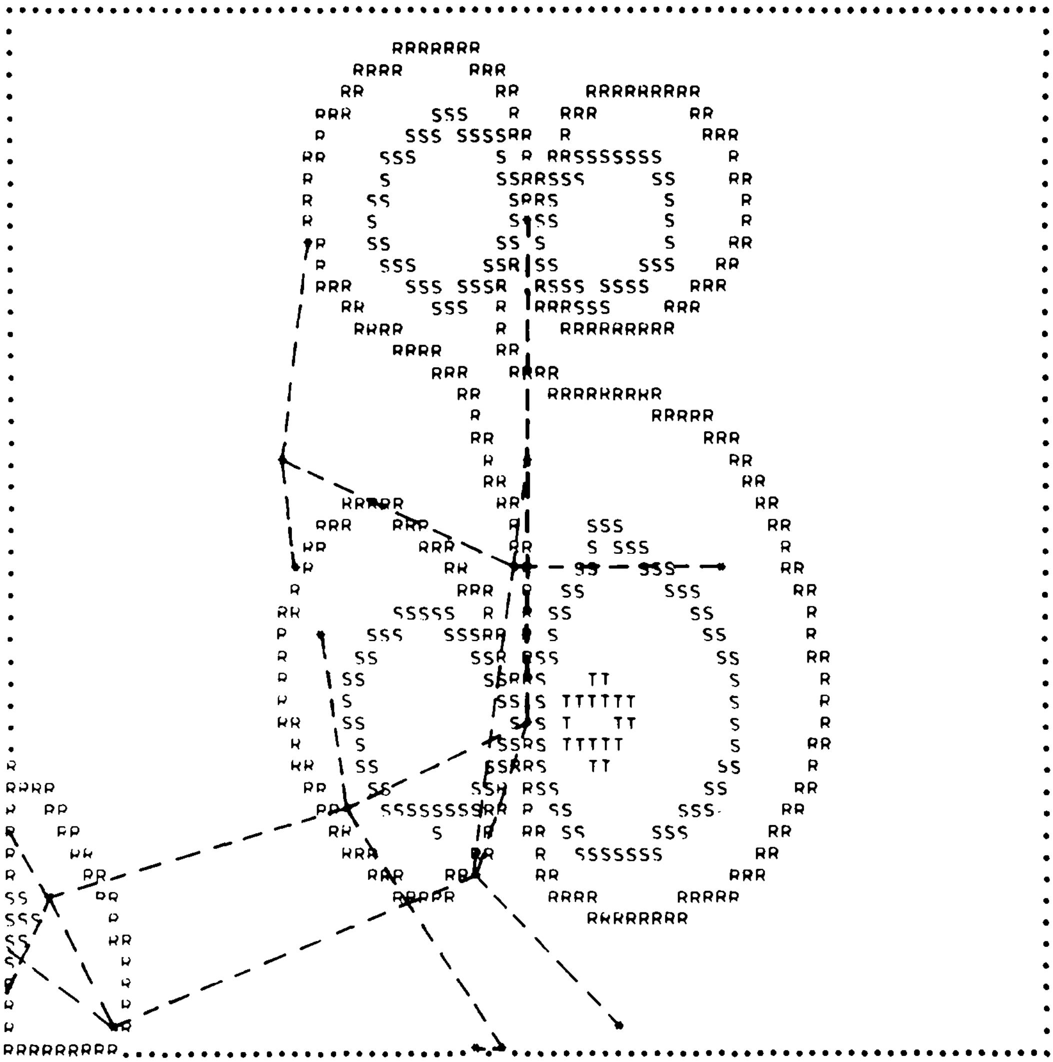

Fig. 7. Electron density maps of the NNHOMO (MO 32) of 7-$NH_2$-3$\alpha$-COOH-penam (S)-sulfoxide from EH calculations. This view shows the density computed in the same plane as Fig. 6.

equatorial position and that the (S)-sulfoxide is more stable than the (R)-sulfoxide. The latter finding follows from the possibility of intramolecular H-bonding[30] between the 6-acylamido N–H and the $\beta$ face sulfoxide oxygen because the H···O distance can be about 1.9 Å. EH MO theory works fairly well at representing some hydrogen bonding situations, but does poorly at others.[8,31] Of the zwitterionic 6-APA sulfoxide models 3 and 4, the (R)-sulfoxides are calculated to be more stable by a few kcal/mole, thus showing up the inability of the EH method to yield a H-bond stabilization here. However, the Mulliken overlap population of about 0.015 between the sulfoxide $O_{13}$ and one H on the -$NH_3^+$ group and the increased positive net atomic charge on that H (+0.23 vs +0.21 or +0.22 on the other -$NH_3^+$ protons) are indicative of some interaction in 4. The thiazolidine ring conformation with the 3$\alpha$-$COO^-$ equatorial is predicted to be 2.5 kcal/mole less stable than the axial conformer in the (R)-sulfoxide model, but 1.3 kcal/mole more stable in the (S)-sulfoxide. Only the latter result seems to be consistent with the data on penicillin sulfoxides.[30] A theoretical method more reliable than the EH method, such as the force field method recently developed for sulfoxides and applied effectively to 6-membered ring structures,[32] seems to be required to understand the fascinating conformational preferences of penam sulfoxides.

*Acknowledgements*—We are grateful to the following for their contributions: M. M. Marsh and R. D. Miller for making available to us their unpublished spectral data and for discussions, T.-S. Chou for generously supplying a sample of 6-APA (S)-sulfoxide, N. L. Allinger, R. R. Chauvette, D. E. Dorman, R. B. Hermann, R. Hoffmann, S. P. Kukolja and D. O. Spry for helpful comments. M. A. Bogan and T. K. Elzey for technical assistance, and R. W. Counts for making QCPE 279 and 309 available to us as soon as possible. The computer calculations done at the University of Virginia were supported by the National Science Foundation (through a grant to F.R.) and by the Camille and Henry Dreyfus Foundation (through a Teacher-Scholar Award to F.R.).

*Note added in proof*: In an exchange of preprints with H. Vanderhaeghe after this paper had been submitted, we became aware of CD studies on some novel and very interesting penams, penam (R)- and (S)-sulfoxides, and penam sulfones, which had been presented by R. Busson, E. Roets, and H. Vanderhaeghe at the Symposium on Recent Advances in the Chemistry of $\beta$-Lactam Antibiotics, Cambridge, England, June 28–30, 1976. Although they did not study 6-APA (S)-sulfoxide, their spectra for other

(S)-sulfoxides agree quite well qualitatively with ours in Fig. 2. Their discovery that the 230 nm CD band splits into two overlapping bands in some $6\alpha$-substituted penams appears to fit well with our calculations which have predicted two closely-spaced transitions contributing to this band. Their data add further support to the conclusion that the 3-carboxyl group of penams adds little to the CD spectra. Although an alternative interpretation of the 203- and 230-nm CD bands was given in their preliminary presentation, we feel that our data for the amide $\pi \rightarrow \pi^*$ and $n \rightarrow \pi^*$ couplet and for the pH-dependence of these bands point toward the plausibility of our assignments. Our calculated predictions, while clearly not all infallible, do show it is possible to oxidize the sulfur of penam and still not greatly alter the positive CD band at 230 nm. It is conceivable that in going from the sulfide to the sulfoxide to the sulfone that the large changes they observed in the 203-nm band are due to the strong electric dipole of the S–O bonds perturbing the nearby amide orbitals of the $\beta$-lactam ring. Also, their observations of significant disturbance of the characteristic 230-nm band by a $6\alpha$-Cl substituent on penams suggests that this band, as we believe, is not localized on the sulfur functionality. No doubt Professor Vanderhaeghe's forthcoming data will provide a more complete foundation on which to draw conclusions, and we thank him for sharing with us his preprint.

## REFERENCES

[1] D. B. Boyd, C.-Y. Yeh and F. S. Richardson, *J. Am. Chem. Soc.* **98**, 6100 (1976).

[2] D. B. Boyd, *J. Phys. Chem.* **78**, 2604 (1974).

[3] R. D. G. Cooper, L. D. Hatfield and D. O. Spry, *Accounts Chem. Res.* **6**, 32 (1973); S. Kukolja, S. R. Lammert, M. R. Gleissner and A. I. Ellis, *J. Am. Chem. Soc.* **97**, 3192 (1975); P. G. Sammes, *Chem. Rev.* **76**, 113 (1976); and refs cited therein.

[4] D. B. Boyd, *J. Am. Chem. Soc.* **94**, 6513 (1972).

[5] H. Bock and B. Solouki, *Angew. Chem.* Int. Ed. **11**, 436 (1972).

[6] R. Hoffmann, H. Fujimoto, J. R. Swenson and C.-C. Wan, *J. Am. Chem. Soc.* **95**, 7644 (1973); M. H. Palmer and R. H. Findlay, *J. Chem. Soc.* Perkin II, 1223 (1975); M.-M. Rohmer and B. Roos, *J. Am. Chem. Soc.* **97**, 2025 (1975).

[7] R. Hoffmann, *J. Chem. Phys.* **39**, 1397 (1963).

[8] D. B. Boyd and W. N. Lipscomb, *J. Theor. Biol.* **25**, 403 (1969).

[9] J. Webb, R. W. Strickland and F. S. Richardson, *Tetrahedron* **29**, 2499 (1973); F. S. Richardson and R. W. Strickland, *Ibid.* **31**, 2309 (1975); C.-Y. Yeh and F. S. Richardson, *J. Chem. Soc.* Faraday II, 331 (1976); C.-Y. Yeh and F. S. Richardson, *Inorg. Chem.* **15**, 682 (1976); and refs cited therein.

[10] L.-H. Hase, H. Meyer and A. Schweig, *Z. Naturforsch.* **29A**, 361 (1974).

[11] D. B. Boyd, *J. Phys. Chem.* **78**, 1554 (1974); D. B. Boyd, *J. Am. Chem. Soc.* **94**, 64 (1972).

[12] W. L. Jorgensen and L. Salem, *Organic Chemist's Book of Orbitals*. Academic Press, New York (1973).

[13] R. C. Bingham, M. J. S. Dewar and D. H. Lo, *J. Am. Chem. Soc.* **97**, 1285, 1294, 1302, 1307 (1975); M. J. S. Dewar, D. H. Lo and C. A. Ramsden, *Ibid.* **97**, 1311 (1975).

[14] D. B. Boyd, *J. Chem. Educ.* **53**, 483 (1976).

[15] J. A. Pople and M. Gordon, *J. Am. Chem. Soc.* **89**, 4253 (1967).

[16] W. C. Krueger and L. M. Pschigoda, *Anal. Chem.* **43**, 675 (1971).

[17] J. Steinhardt and S. Beychok, *Proteins* (Edited by H. Neurath), Vol. II, p. 140. Academic Press, New York (1964).

[18] *Documentation of Molecular Spectroscopy, UV Atlas of Organic Compounds*, Vol. 4, Plates B10/6, 7. Plenum Press, New York (1968).

[19] I. Z. Siemion, J. Lisowski, B. Tyran and J. Morawiec, *Bull. Acad. Pol. Sci., Ser. Sci. Chim.* **20**, 549 (1972).

[20] L. A. Mitscher, P. W. Howison and T. D. Sokoloski, *J. Antibiot.* **27**, 215 (1974).

[21] R. Hoffmann and R. B. Davidson, *J. Am. Chem. Soc.* **93**, 5699 (1971).

[22] C. C. Levin, R. Hoffmann, W. J. Hehre and J. Hudec, *J. Chem. Soc.* Perkin II, 210 (1973).

[23] N. L. Allinger, J. C. Tai and M. A. Miller, *J. Am. Chem. Soc.* **88**, 4495 (1966).

[24] H. A. Bent, *Chem. Rev.* **61**, 275 (1961).

[25] J. A. Schellman, *Accounts Chem. Res.* **1**, 144 (1968).

[26] R. B. Hermann, *J. Am. Chem. Soc.* **91**, 3152 (1969).

[27] J. Lisowski, I. Z. Siemion and B. Tyran, *Rocz. Chem.* **47**, 2035 (1973).

[28] D. B. Boyd, *J. Med. Chem.* **16**, 1195 (1973).

[29] H. Ogura, K. Takeda and H. Takahashi, *Chem. Pharm. Bull.* **23**, 2469 (1975); H. Ogura, H. Takayanagi, K. Kubo and K. Furuhata, *J. Am. Chem. Soc.* **95**, 8056 (1973); H. Ogura, H. Takayanagi and K. Furuhata, *J. Chem. Soc.* Perkin I, 665 (1976); see also, H. Rehling and H. Jensen, *Tetrahedron Lett.*, 2793 (1972).

[30] R. D. G. Cooper, P. V. Demarco, J. C. Cheng and N. D. Jones, *J. Am. Chem. Soc.* **91**, 1408 (1969); R. D. G. Cooper, P. V. Demarco and D. O. Spry, *Ibid.* **91**, 1528 (1969); D. H. R. Barton, F. Comer and P. G. Sammes, *Ibid.* **91**, 1529 (1969); R. A. Archer and P. V. Demarco, *Ibid.* **91**, 1530 (1969); D. O. Spry, *Ibid.* **92**, 5006 (1970); R. A. Archer, R. D. G. Cooper, P. V. Demarco and L. F. Johnson, *J. Chem. Soc.* Chem. Commun. 1291 (1970); R. D. G. Cooper and D. O. Spry, *Cephalosporins and Penicillins: Chemistry and Biology* (Edited by E. H. Flynn), p. 183. Academic Press, New York (1972); P. V. Demarco and R. Nagarajan, *Ibid.*, p. 311; A. K. Bose, B. Dayal, H. P. S. Chawla and M. S. Manhas, *Tetrahedron* **28**, 5977 (1972); A. J. Vlietinck, E. Roets, H. Vanderhaeghe and S. Toppet, *J. Org. Chem.* **39**, 441 (1974); C. M. Dobson, L. O. Ford, S. E. Summers and R. J. P. Williams, *J. Chem. Soc.* Faraday II **71**, 1145 (1975); C. R. Harrison and P. Hodge, *J. CHEM. Soc.* Perkin I, 1772 (1976).

[31] L. B. Kier, *Molecular Orbital Theory in Drug Research*. Academic Press, New York (1971); J. R. Hoyland, *Molecular Orbitals in Chemical Pharmacology* (Edited by L. B. Kier), p. 31. Springer-Verlag, New York (1970); A. S. N. Murthy and C. N. R. Rao, *Chem. Phys. Lett.* **2**, 123 (1968); P. A. Kollman and L. C. Allen, *Chem. Rev.* **72**, 283 (1972); C. N. R. Rao, P. C. Dwivedi, A. Gupta, H. S. Randhawa, H. Ratajczak, M. M. Szczesniak, K. Romanowska and W. J. Orville-Thomas, *J. Mol. Structure* **30**, 271 (1976).

[32] N. L. Allinger and J. Kao, *Tetrahedron* **32**, 529 (1976).